Appl. Num. Anal. Comp. Math. **1**, No. 2, 343 – 352 (2004) / **DOI** 10.1002/anac.200410002

Region and Contour Identification of Physical Objects

Annie Cuyt[1], **Jan Sijbers**[2], **Brigitte Verdonk**[1], and **Dirk Van Dyck**[2]

[1] Universiteit Antwerpen, Departement Wiskunde en Informatica, Middelheimlaan 1, B-2020 Antwerpen, Belgium
{annie.cuyt@ua.ac.be, brigitte.verdonk@ua.ac.be}

[2] Universiteit Antwerpen, Departement Fysica, Groenenborgerlaan 171, B-2020 Antwerpen, Belgium
{jan.sijbers@ua.ac.be, dirk.vandyck@ua.ac.be}

Received 1 December 2004, revised 6 December 2004, accepted 6 December 2004
Published online 20 December 2004

The region occupied by and the contour of a physical object in 3-dimensional space are in a way dual or interchangeable characteristics of the object: the contour is the region's boundary and the region is contained inside the contour. In the same way the characterization of the object's contour by its Fourier descriptors, and the reconstruction of its region from the object's multidimensional moments, are also dual problems. While both problems are well-understood in two dimensions, the complexity increases tremendously when moving to the three-dimensional world.

In Section 2 we discuss how the latest techniques allow to reconstruct an object's shape from the knowledge of its moments. For 2D significantly different techniques must be used, compared to the general 3D case.

In Section 3, the parameterization of a 2D contour onto a unit circle and a 3D surface onto a unit sphere is described. Furthermore, the theory of Fourier descriptors for 2D shape representation and the extension to 3D shape analysis are discussed.

The reader familiar with the use of either Fourier descriptors or moments as shape descriptors of physical objects may find the comparative discussion in the concluding section interesting.

1 Introduction

The problems of shape characterization and reconstruction of an object from measured data are ubiquitous in computational science and engineering. Applications can be found in meteorology, medicine, space exploration, manufacturing, entertainment and defense, to name just a few. In this paper, we focus on Fourier descriptors for shape characterization and on moments for shape reconstruction. Both magnitudes are interrelated by many mathematical formulas, among which several involving integral transforms.

Digital representations of volumetric objects usually consist of a large number of binary volume elements or a polygonized surface. In practice these representations lack descriptive power as they are based on huge lists of voxels or surface elements [4]. Effective characterization of the represented shape requires a limited number of shape descriptors, meaning measurable or computable object features. Contour-based shape descriptors, such as Fourier descriptors, exploit only boundary information and cannot capture the shape interior nor deal with disjoint shapes. In region based techniques, such as moment based techniques, information across an entire object rather than just at boundary points is combined.

Fourier descriptors are widely used in 2D as well as 3D. Characterization or recognition of objects by means of Fourier descriptors has extensively been described in the past, especially in 2D [55, 41, 38, 50, 29, 42, 34]. During the past fifteen years, Fourier descriptors were also employed for 3D applications, such as the recognition of 3D curves [9, 51], or recognition of 3D objects from projections or 2D slices [52, 2, 15, 30]. Finally, Fourier descriptors for shape description and recognition can be constructed directly from 2D manifolds in a 3D space [27, 46, 4, 6, 53, 54]. Application areas of Fourier descriptors range from cell biology, medicine [28, 31], to aviation [41, 29], character recognition [38] and watermarking [45].

In many instances of shape reconstruction, indirect object measurements of the underlying shape can be distilled into moments. Such inverse moment problems appear in diverse areas, among which probability and statistics [14], signal processing [43], heat conduction [1], computed tomography [35, 36] and magnetic and gravitational anomaly detection [8, 47]. Besides in shape reconstruction, moment based techniques have also extensively been used in imagery for image analysis and object representation or recognition [25, 33, 32, 37, 40, 49, 48, 56]. For such applications, the invariance to translation, rotation and scaling is essential.

Both Fourier descriptors and multidimensional moments can be made invariant to translation, rotation and scaling of the object under investigation. For 2D Fourier descriptors this is achieved by dividing all Fourier coefficients by the Fourier coefficient indexed by zero and ignoring the phases. Moment invariants insensitive to the same transformations are obtained by first computing their central and aspect ratio invariant form and then combining these into rotation invariant expressions. The transformation invariance of these parameters, extracted either from the object's contour or its overall region, makes them tractable shape descriptors. However, for the applications under investigation in this paper, the transformation invariance is not required.

In this paper, the latest techniques to reconstruct an object's shape from the knowledge of its moments is discussed and the theory of Fourier descriptors for shape representation is reviewed. For both topics the non-trivial extension from 2D to 3D shape analysis is discussed.

2 Moment information

Let us first describe how the problem of identifying a shape from its moments is dealt with in two dimensions. Since both variables are real, the problem can also be viewed as a one-dimensional problem in a complex variable. Therefore, the complexity of the two-dimensional formulation is not representative for that of the higher dimensional problem in general.

2.1 2D reconstruction

In case the object is a polygon [18], or when it defines a quadrature domain in the complex plane [21], its shape can be reconstructed from the knowledge of its moments, using a connection between formally orthogonal polynomials and numerical quadrature. We summarize the polygonal case because it allows an exact reconstruction.

Let $\{c_k\}_{k\in\mathbb{N}}$ denote the sequence of moments of the polygon $P \subset \mathbb{C}$,

$$c_k = \int\int_P (x + \mathrm{i}y)^k \, dx \, dy \tag{1}$$

and let us define linear functionals c and $c^{(n)}$ from the vector space $\mathbb{C}[z]$ to $\mathbb{C}$ by

$$\begin{aligned} c(z^k) &= c_k \qquad && k \geq 0 \\ c^{(n)}(z^k) &= c_{k+n} \qquad && n \geq 0, k \geq 0 \end{aligned}$$

In the sequel we set $c_k = 0$ when $k < 0$. With the sequence $\{c_k\}_{k\in\mathbb{N}}$ we also associate the Hankel matrices

$$H_m^{(n)} = \begin{pmatrix} c_n & \cdots & c_{n+m-1} \\ \vdots & \iddots & c_{n+m} \\ & & \vdots \\ c_{n+m-1} & \cdots & c_{n+2m-2} \end{pmatrix} \qquad H_0^{(n)} = 1 \tag{2}$$

and

$$H_m^{(n)}(z) = \begin{pmatrix} c_n & \cdots & c_{n+m-1} & c_{n+m} \\ \vdots & \iddots & & \\ & & \vdots & \vdots \\ c_{n+m-1} & \cdots & & c_{n+2m-1} \\ 1 & \cdots & z^{m-1} & z^m \end{pmatrix} \qquad H_0^{(n)}(z) = 1 \tag{3}$$

and the Hadamard polynomials

$$p_m^{(n)}(z) = \frac{\det H_m^{(n)}(z)}{\det H_m^{(n)}} \qquad m \geq 0, n \geq 0 \tag{4}$$

These monic polynomials of degree m are formally orthogonal with respect to the linear functional $c^{(n)}$ because they satisfy [7, pp. 40–41]

$$c^{(n)}\left(z^i p_m^{(n)}(z)\right) = 0 \qquad i = 0, \ldots, m-1$$

The functional c is called m-normal if

$$\det H_i^{(n)} \neq 0 \qquad n \geq 0 \qquad i = 0, \ldots, m$$

If the moments c_k are not given by (1), but by

$$c_k = k(k-1) \int\int_P (x + \mathrm{i}y)^{k-2}\, dx\, dy \tag{5}$$

then the zeroes of the Hadamard polynomial $p_m^{(0)}(z)$ are precisely the m vertices of the polygon P [18]. This property is based on the following quadrature result from [12, 13].

Theorem 2.1 *Let $z_1, \ldots, z_m$ denote the vertices of a polygon P in the complex plane and let $f(z)$ be a function analytic in the closure of P. Then there exist constants $a_1, \ldots, a_m$ depending upon $z_1, \ldots, z_m$ but independent of f, such that*

$$\int\int_P f''(z)\, dx\, dy = \sum_{j=1}^{m} a_j f(z_j) \tag{6}$$

If the region P is unknown but its complex moments c_k are known from (5), then (6) with $f(z) = z^k$ for $k \geq 2$, can be seen as a means to determine the z_j and a_j that characterize P.

The zeroes of $p_m^{(0)}(z)$ can be obtained by solving the generalized eigenvalue problem

$$H_m^{(1)} u = z H_m^{(0)} u$$

where u denotes a vector in $\mathbb{C}^m$. The solution of this generalized eigenvalue problem can be obtained most stably by the QZ algorithm, which can be improved as in [18] because of the special form of $H_m^{(0)}$ and $H_m^{(1)}$. The replication of columns of $H_m^{(0)}$ in $H_m^{(1)}$ allows to compute the QR factorization of $H_m^{(0)}$ augmented by the last column of $H_m^{(1)}$. This brings $H_m^{(0)}$ in triangular form and $H_m^{(1)}$ in upper Hessenberg form, as required.

After determining the vertices z_j, the coefficients a_j in the quadrature result can be computed from

$$\begin{pmatrix} 1 & 1 & \ldots & 1 \\ z_1 & z_2 & \ldots & z_m \\ \vdots & \vdots & \ddots & \vdots \\ z_1^{m-1} & z_2^{m-1} & \ldots & z_m^{m-1} \end{pmatrix} \begin{pmatrix} a_1 \\ \vdots \\ \\ a_m \end{pmatrix} = \begin{pmatrix} c_0 \\ \vdots \\ \\ c_{m-1} \end{pmatrix}$$

Then the interior of the polygon has to be reconstructed. This is important in case the polygon is not assumed to be convex [36]. In [18] it is indicated how the conditioning can be improved by using so-called transformed moments with respect to a shifted and scaled basis. For a numerical illustration of the above technique we refer to [18].

2.2 3D reconstruction

Since an analogue of Theorem 2.1 does not exist in higher dimensions, another approach must be followed in three real dimensions. The Hadamard polynomial $p_m^{(n)}(z)$ is also connected to Padé approximation theory by the following. Given a series of the form

$$g(z) = \sum_{i=0}^{\infty} (-1)^i c_i z^i \tag{7}$$

the Padé approximant $r_{m-1,m}(z) = p_{m-1,m}(z)/q_{m-1,m}(z)$ to $g(z)$ of degree $m-1$ in the numerator and m in the denominator is computed from the conditions

$$p_{m-1,m}(z) = \sum_{i=0}^{m-1} a_i z^i \qquad q_{m-1,m}(z) = \sum_{i=0}^{m} b_i z^i \tag{8}$$

$$\left(\sum_{i=0}^{\infty} (-1)^i c_i z^i\right) q_{m-1,m}(z) - p_{m-1,m}(z) = \sum_{i=0}^{\infty} d_i z^{2m+i} \tag{9}$$

An explicit formula for the Padé denominator $q_{m-1,m}(z)$ is given by

$$q_{m-1,m}(z) = z^m \, p_m^{(m-1)}(1/z)$$

Now let $g(z)$ be a Markov function, meaning that $g(z)$ is defined to be a function with the integral representation

$$g(z) = \int_a^b \frac{f(u)}{1+zu}\, du \qquad z \notin]-\infty, -1/b] \cup [-1/a, +\infty[\tag{10}$$

$$-\infty < a \le 0 \le b < +\infty \tag{11}$$

where $f(u) \ge 0$, and the coefficients c_i are the moments of f

$$c_i = \int_a^b f(u)\, u^i \, du \tag{12}$$

Then the following convergence result for Padé approximants holds [3, p. 228].

Theorem 2.2 *The sequence* $\{r_{m-1,m}(z)\}_{m\in\mathbb{N}}$ *of Padé approximants to the Markov function* (10) *converges to* (10) *for* $z \notin]-\infty, -1/b] \cup [-1/a, +\infty[$. *The rate of convergence is governed by*

$$\limsup_{m\to\infty} |g(z) - r_{m+k,m}(z)|^{1/m} \le \left| \frac{\sqrt{1/z+b} - \sqrt{1/z+a}}{\sqrt{1/z+b} + \sqrt{1/z+a}} \right|$$

Fortunately a multivariate generalization of the concept of Padé approximant exists that allows a convergence result like the one in Theorem 2.2. A trivariate Stieltjes function $g(v, w, z)$ is defined by the integral representation

$$g(v,w,z) = \int_0^\infty \int_0^\infty \int_0^\infty \frac{f(t,s,u)}{1+(vt+ws+zu)}\, dt\, ds\, du \tag{13}$$

with $f(t, s, u) \ge 0$ and finite real-valued moments

$$c_{ijk} = \int_0^\infty \int_0^\infty \int_0^\infty t^i s^j u^k f(t,s,u)\, dt\, ds\, du$$

A formal expansion of (13) provides a trivariate Stieltjes series of the form

$$g(v,w,z) = \sum_{i,j,k=0}^{\infty} (-1)^{i+j+k} \binom{i+j+k}{i+j} \binom{i+j}{i} c_{ijk} v^i w^j z^k \tag{14}$$

Given (14) one can compute the $(m-1, m)$ homogeneous trivariate Padé approximant to (14) as follows. First, we introduce the homogeneous expressions

$$A_\ell(v,w,z) = \sum_{i+j+k=\ell} a_{ijk} v^i w^j z^k$$

$$B_\ell(v,w,z) = \sum_{i+j+k=\ell} b_{ijk} v^i w^j z^k$$

and define the polynomials

$$p_{m-1,m}(v,w,z) = \sum_{\ell=(m-1)m}^{(m-1)m+m-1} A_\ell(v,w,z)$$
$$q_{m-1,m}(v,w,z) = \sum_{\ell=(m-1)m}^{(m-1)m+m} B_\ell(v,w,z)$$

Then, with

$$C_\ell(v,w,z) = \sum_{i+j+k=\ell} \binom{i+j+k}{i+j}\binom{i+j}{i} c_{ijk} v^i w^j z^k \qquad (15)$$

we write down the homogeneous accuracy-through-order conditions

$$\left(\left(\sum_{\ell=0}^{\infty}(-1)^\ell C_\ell\right) q_{m-1,m} - p_{m-1,m}\right)(v,w,z) = \sum_{i+j+k=m(m-1)+2m}^{\infty} d_{ijk}\, v^i\, w^j\, z^k \qquad (16)$$

It has been shown [10, pp. 60–61] that a nontrivial solution for $p_{m-1,m}(v,w,z)$ and $q_{m-1,m}(v,w,z)$ can always be computed from (16). Moreover, all solutions $p_{m-1,m}(v,w,z)/q_{m-1,m}(v,w,z)$ deliver the same unique irreducible form $r_{m-1,m}(v,w,z)$ which is called the homogeneous Padé approximant to (14). This multivariate generalization of the concept of Padé approximant is the one most closely related to the univariate Padé approximant because of the following projection property. Let, for particular $-\pi \le \theta \le \pi$ and $0 \le \phi \le \pi/2$, the one-dimensional subspace $S_{\theta,\phi} \subset \mathbb{R}^3$ be given by

$$S_{\theta,\phi} = \{(z\cos\phi\cos\theta, z\cos\phi\sin\theta, z\sin\phi) \mid z \in \mathbb{R}\}$$

and denote the restriction of $r_{m-1,m}(v,w,z)$ to $S_{\theta,\phi}$ by $r_{m-1,m}^{(\theta,\phi)}(z)$. When projecting the homogeneous polynomials $C_\ell(v,w,z)$ given by (15) on $S_{\theta,\phi}$, we find

$$\begin{aligned} C_\ell(z\cos\phi\cos\theta, &z\cos\phi\sin\theta, z\sin\phi) \\ &= \sum_{i+j+k=\ell} \binom{i+j+k}{i+j}\binom{i+j}{i} c_{ijk}(\cos\phi\cos\theta)^i(\cos\phi\sin\theta)^j(\sin\phi)^k z^\ell \\ &= C_\ell(\cos\phi\cos\theta,\cos\phi\sin\theta,\sin\phi)z^\ell \end{aligned}$$

Replacing c_i in (4) by $C_i(\cos\phi\cos\theta,\cos\phi\sin\theta,\sin\phi)$, parameterizes the Hadamard polynomial $p_m^{(m-1)}(z)$ by θ and ϕ. We however don't want to burden the notation for $p_m^{(m-1)}(z)$ with two additional parameters. An explicit formula for the Padé denominator $q_{m-1,m}(v,w,z)$ restricted to $S_{\theta,\phi}$ can be given in terms of this parameterized Hadamard polynomial:

$$q_{m-1,m}(z\cos\phi\cos\theta, z\cos\phi\sin\theta, z\sin\phi)/z^{m(m-1)} = z^m p_m^{(m-1)}(1/z)$$

A more general determinant representation also holds [10, p. 17]. The above projection property makes it possible to compute the overall approximant $r_{m-1,m}(v,w,z)$ for $g(v,w,z)$ and subsequently apply Theorem 2.2 on every slice $S_{\theta,\phi}$ [11]. When $f(t,s,u)$ in (13) is the characteristic function of the object A, appropriately scaled, and a number of moments c_{ijk} of A is given, then:

- the left-hand side of (13) can be obtained and evaluated at several (v_ℓ, w_ℓ, z_ℓ) in the unit ball, through its Padé approximant $r_{m-1,m}(v,w,z)$ of sufficiently high degree;
- the right-hand side of (13) can be discretized using a cubature rule for the unit ball, which leads to a linear system in the unknowns $f(t_h,s_h,u_h)$ where each (t_h,s_h,u_h) is a node of the cubature rule;

- the resulting linear system, which is ill-posed [22], can be regularized using the truncated SVD algorithm and then solved for the $f(t_h, s_h, u_h)$.

Besides reconstructing three-dimensional objects A the above technique can also be used for the reconstruction of non-polygonal 2D shapes. Several examples of both 2D and 3D reconstructed objects can be found in [11].

3 Fourier descriptors

Fourier descriptors are widely used in shape description and recognition problems. An essential preprocessing step to be carried out before the actual computation of the Fourier coefficients and Fourier descriptors is the discrete parameterization of the given contour. In particular, a 2D contour must be mapped onto a circle, after which it can be expanded into elliptical harmonic functions. In 3D, a surface must be mapped onto a sphere, after which it can be expanded into spherical harmonic functions. As is explained in the next sections, the latter is all but trivial compared to the 2D analogon.

Fourier descriptors are particularly valuable for parameterizations that exhibit periodicity and that can be modelled by means of a limited number of Fourier functions.

3.1 2D parameterization

The boundary of a simply connected two-dimensional region is a closed contour. The simplest closed contour that shares the same topology as an arbitrary closed contour is the unit circle

$$\mathbb{S}^1 = \{z \in \mathbb{C} : |z|^2 = 1\} \tag{17}$$

and $\mathbb{S}^1$ is therefore an adequate parameter space. The mapping of the 2D contour onto the unit circle is trivial. Indeed, if the contour has N pixels, then N points can be equally distributed over the unit circle. The locations of these points are given by $(\cos\phi_n, \sin\phi_n)$ with $\phi_n = 2\pi n/N$. Hence, the polar coordinate ϕ_n parameterizes the contour. By traversing the contour in object space, the unit circle is traversed as well at a constant speed. Each angle ϕ_n corresponds to a unique point (x_n, y_n) on the contour. Note that the contour is a periodic function of ϕ_n. Hence, the harmonic functions are the preferred set of basis functions.

It is important to note that the sampling of the unit circle must be uniform. If this uniformity is not met, the orthogonality relation of the Fourier basis functions evaluated in discrete points on the unit circle, does not hold, which results in erroneous Fourier descriptors.

3.2 3D parameterization

Similar to parameterization in 2D, a surface can be mapped onto a unit sphere. In 3D, however, no direction or order exists. During the past ten years, various methods were proposed to deal with this mapping problem. An interesting approach to map a polyhedron onto a sphere has been proposed in [4] where a continuous one-to-one mapping from the surface of the original object to the surface of a unit sphere is proposed. Thereby, two poles are selected on the surface, after which the vertices are uniformly mapped onto the sphere by means of a diffusion process. Because of this diffusion process, however, the algorithm may be a computational burden, especially for polygon models with a large number of vertices. The mapping procedure can be improved based on the use of progressive meshes [24, 44, 39, 19, 20].

A progressive mesh is a multi-resolution representation of a mesh in which edges are iteratively collapsed based on a chosen criterion [16]. In [17, 23] a fast and efficient method to obtain a multi-resolutional representation of a polyhedron using a quadric error metric is developed [17, 23]. During the simplification, vertex pairs are iteratively contracted such that this quadric error is minimal. Simplification of the polyhedron is continued until only a few vertices remain. Thereby, constraints are imposed on the simplification scheme so as to ensure that the topology is not changed. After the construction of the progressive mesh, the strongly simplified polyhedron is mapped onto the unit sphere, after which iterative reconstruction is performed on the sphere.

Mapping of 3D surfaces to a parameter domain is an essential preprocessing step. At the moment, efficient parameterization methods are avaliable to map genus-0 objects onto a sphere. However, depending on the object's shape, other parameterization domains may be more suitable. As indicated in [26], tubular objects are more suited to be parameterized on a cylinder. Also, objects with a higher genus should be mapped onto the appropriate domain. For example, a genus-1 object (closed object with one hole) has a donut-like shape as its natural parameterization domain. Developing a suitable parameterization for each surface type is a challenge.

3.3 2D Fourier descriptors

A closed contour C in 2D can be represented by a complex function $z(t)$, where $z(t) = x(t) + \mathrm{i}y(t)$. Thereby, $x(t)$ and $y(t)$ represent the x- and y-coordinates of the contour points. If z is periodic with period T, i.e. $z(t) = z(t + kT)$, expansion of $z(t)$ into a Fourier series yields

$$z(t) = \sum_{n=-\infty}^{\infty} a_n \exp\left(\frac{2\pi\mathrm{i}nt}{T}\right) \tag{18}$$

where the Fourier coefficients are found from the Fourier transform of $z(t)$:

$$a_n = \int_0^T z(t) \exp\left(\frac{-2\pi\mathrm{i}nt}{T}\right) dt \tag{19}$$

If the contour is sampled on a discrete grid, the discrete Fourier transform of $z(t)$ is given by

$$a_n = \frac{1}{N} \sum_{t=0}^{N-1} z(t) \exp\left(-\mathrm{i}\phi_n t\right) \qquad \phi_n = \frac{2\pi n}{N} \tag{20}$$

Subsequently, the Fourier coefficients a_n are appropriately transformed to make them independent to translation, rotation, scale, and starting point, by dividing all coefficients a_n by a_0 and ignoring the phases.

3.4 3D Fourier descriptors

Consider a 3D closed object, of which the surface is described by an object function $\boldsymbol{r}(x, y, z)$. A suitable parameterization domain for a closed surface is the unit sphere $\mathbb{S}^2$, since they share the same topology. The parameterization defines the relation between the coordinates $\boldsymbol{n}(\theta, \phi) = (\cos\phi\cos\theta, \cos\phi\sin\theta, \sin\phi)^T$ of points located on the unit sphere and the coordinates on the object's surface:

$$\boldsymbol{S}(\theta, \phi) = \begin{pmatrix} x(\theta, \phi) \\ y(\theta, \phi) \\ z(\theta, \phi) \end{pmatrix} \tag{21}$$

Now assume that N observations are available at the locations $\boldsymbol{n}_i, i = 1, \ldots, N$. Then $\boldsymbol{S}(\theta, \phi)$ at a new location $\boldsymbol{n}(\theta, \phi)$ can be approximated from the observations $\boldsymbol{S}(\theta_i, \phi_i)$ using the spherical harmonic functions Y_ℓ^m:

$$\boldsymbol{S}(\theta, \phi) \approx \widehat{\boldsymbol{S}}(\theta, \phi) = \sum_{\ell=0}^{L} \sum_{m=-\ell}^{\ell} \boldsymbol{a}_\ell^m Y_\ell^m(\theta, \phi) \tag{22}$$

where the Fourier coefficients $\boldsymbol{a}_\ell^m$ are the inner product of the vector $\boldsymbol{S}$ with the spherical harmonic function Y_ℓ^m:

$$\boldsymbol{a}_\ell^m = \langle \boldsymbol{S}, Y_\ell^m \rangle = \int_0^{2\pi} \int_0^{\pi} \boldsymbol{S}(\theta, \phi) Y_\ell^m(\theta, \phi) \sin\theta d\theta d\phi \tag{23}$$

In practical applications, these coefficients are often estimated by a least squares fitting of the spherical harmonics to the discrete observations:

$$\widehat{\boldsymbol{a}} = \sum_{i=1}^{N} \boldsymbol{S}(\theta_i, \phi_i) \boldsymbol{y}^H(\theta_i, \phi_i) (\boldsymbol{Y}^H \boldsymbol{Y})^{-1} \tag{24}$$

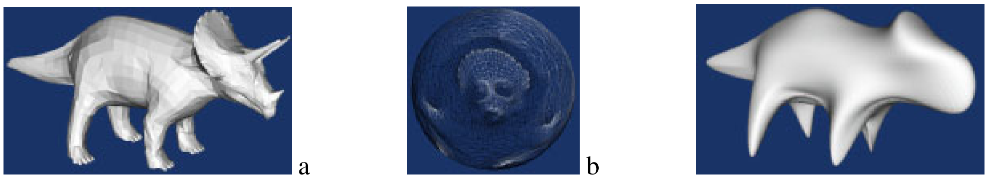

a b c

Fig. 1 a) original mesh b) spherical mapping c) limited Fourier reconstruction

where $\boldsymbol{y}(\theta,\phi) = [Y_0^0(\theta,\phi), Y_1^{-1}(\theta,\phi), Y_1^0(\theta,\phi), Y_1^1(\theta,\phi), ..., Y_L^L(\theta,\phi)]^T$ and $\boldsymbol{Y} = [\boldsymbol{y}(\theta_1,\phi_1), ..., \boldsymbol{y}(\theta_N,\phi_N)]^T$. Note that the above equation simplifies significantly in case the observations are regularly spaced since in that case the discrete version of the orthogonality conditions

$$\int_0^{2\pi}\int_0^{\pi} Y_{\ell'}^{m'}(\theta,\phi)Y_\ell^{m*}(\theta,\phi)\sin\theta d\theta d\phi = \delta_{\ell',\ell}\delta_{m',m} \tag{25}$$

is satisfied, where Y_ℓ^{m*} denotes the complex conjugate of Y_ℓ^m.

By making the Fourier coefficients $\boldsymbol{a}_\ell^m$ invariant to translation, rotation, and scale [4], 3D Fourier descriptors are obtained. Similarly to 2D, translation invariance is achieved by ignoring the component $\boldsymbol{a}_0$. Rotation invariance can be obtained by rotating the object to a standard orientation. Indeed, a representation of the object by only the spherical harmonics of degree 1 is an ellipsoid, which can be aligned along an axis of choice[5]. The same transformation parameters are then applied to the whole object. In case of degeneracy, e.g. when the ellipsoid is a sphere, spherical harmonics of higher degree can be taken into account. Finally, scale invariance can be achieved by dividing all descriptors by the length of the main axis of the ellipsoid.

The computation of 3D Fourier descriptors itself is not fundamentally different from the computation of 2D Fourier descriptors. However, the parameterization step preceeding the computation of Fourier coefficients from surface data is significantly more difficult in 3D than in 2D.

Reconstruction from a limited number of Fourier coefficients allows a multi-resolution approach. In particular, reconstruction from a spherical harmonic with degree 0 yields the sphere that matches the object best in a least squares sense. Similarly, reconstruction from spherical harmonics with maximum order 1 finds the best fitting ellipsoid. The more coefficients are used for the reconstruction, the more detail is added to the reconstruction. An example of a reconstruction of a polyhedron with a limited number of spherical harmonics is shown in Fig. 1.

4 Conclusion

From the sections 2.1, 3.1 and 3.3 the following interplay between Fourier descriptors and moments for closed 2D curves is apparent. Let $z(t) = x(t) + \mathrm{i}y(t)$ describe a closed 2D contour C, bounding a compact 2D area. Let N points be sampled on the contour, thus approximating the curve by a polygonal contour with N vertices. On one hand, if a sufficient number of moments of the polygon are available, namely $2N-1$, Theorem 2.1 enables one to reconstruct the polygonal contour representing $z(t)$. On the other hand, the Fourier coefficients (20) characterize $z(t)$ and can further be used for a variety of applications, among which smoothing, classification and the like.

While the polygonal/polyhedral representation of a physical object continues to play a major role in the computation of 3D Fourier descriptors, this stepping stone can be omitted in 3D shape reconstruction from moments. However, this kind of generality comes at a price. At this moment, it is not possible to reconstruct only the boundary of a 3D object from moment information. One reconstructs the entire area occupied by the object. It is our hope that a better understanding of the interplay between

- techniques for the 3D parameterization of several kinds of objects, and
- formulas expressing moments in terms of shape characteristics such as vertices,

can lead to the removal of this drawback.

References

[1] D.D. Ang, R. Gorenflo, V.K. Le, and D.D. Trong. *Moment theory and some inverse problems in potential theory and heat conduction*. Springer, 2002.

[2] K. Arbter, W.E. Snyder, H. Burkhardt, and G. Hirzinger. Application of affine-invariant Fourier descriptors to recognition of 3-D objects. *IEEE Transactions on Pattern Analysis and Machine Intelligence*, 12(7):640–647, July 1990.

[3] G.A. Baker, Jr. and P. Graves-Morris. *Padé approximants (2nd Ed.)*. Cambridge University Press, 1996.

[4] C. Brechbühler. *Description and analysis of 3D shapes by parameterization of closed surfaces*. PhD thesis, Swiss Federal Institute of Technology Zurich, 1995.

[5] C. Brechbühler, G. Gerig, and O. Kübler. Surface parametrization and shape description. volume 1808, pages 80–89, October 1992.

[6] C. Brechbühler, G. Gerig, and O. Kübler. Parametrization of closed surfaces for 3D shape description. *Comp. Vision and Image Understanding*, 61(2):154–170, 1995.

[7] C. Brezinski. *Padé type approximation and general orthogonal polynomials*. ISNM 50, Birkhauser Verlag, Basel, 1980.

[8] M. Brodsky and E. Panakhov. Concerning a priori estimates of the solution of the inverse logarithmic potential problem. *Inverse problems*, 6:321–330, 1990.

[9] F. S. Cohen and J. Y. Wang. Part I: Modeling image curves using invariant 3D object curve models - a path to 3D recognition and shape estimation from image contours. *IEEE Transactions on Pattern Analysis and Machine Intelligence*, 16(1):1–12, 1994.

[10] A. Cuyt. *Padé approximants for operators: theory and applications*. LNM 1065, Springer Verlag, Berlin, 1984.

[11] A. Cuyt, G. Golub, P. Milanfar, and B. Verdonk. Multidimensional integral inversion, with applications to shape reconstruction. Submitted for publication, 2004.

[12] P. Davis. Triangle formulas in the complex plane. *Math. Comp.*, 18:569–577, 1964.

[13] P. Davis. Plane regions determined by complex moments. *J. Approx. Theory*, 19:148–153, 1977.

[14] P. Diaconis. Application of the method of moments in probability and statistics. In *Proc. Symp. Appl. Math. 37*, pages 125–142. AMS, Providence RI, 1987.

[15] Rocio Diaz de Leon and L. E. Sucar. Human silhouette recognition with Fourier descriptors. In *ICPR00*, volume III, pages 709–712, 2000.

[16] M. Garland. *Quadric-based polygonal surface simplification*. PhD thesis, School of Computer Science, Carnegie Mellon University, May 1999.

[17] M. Garland and P. S. Heckbert. Surface simplification using quadric error metrics. *SIGGRAPH - Computer Graphics*, 1:209–216, 1997.

[18] G.H. Golub, P. Milanfar, and J. Varah. A stable numerical method for inverting shape from moments. *SIAM J. Sci. Comput.*, 21:1222–1243, 1999.

[19] C. Gotsman, X. Gu, and A. Sheffer. Fundamentals of spherical parameterization for 3D meshes. *ACM Transactions on Graphics*, 22, 2003.

[20] X. Gu, Y. Wang, T. Chan, P. Thompson, and S. Yau. Genus zero surface conformal mapping and its application to brain surface mapping. In *Information Processing Medical Imaging 2003*, volume 18, pages 172–184, July 2003.

[21] B. Gustafsson, C. He, P. Milanfar, and M. Putinar. Reconstructing planar domains from their moments. *Inverse Problems*, 16:1053–1070, 2000.

[22] Per Christian Hansen. *Rank-deficient and discrete ill-posed problems*. SIAM Monographs on Mathematical Modeling and Computation. Society for Industrial and Applied Mathematics (SIAM), Philadelphia, PA, 1998. Numerical aspects of linear inversion.

[23] P. S. Heckbert and M. Garland. Optimal triangulation and quadric-based surface simplification. *Computational Geometry - Theory and Application*, 14(1):49–66, 1999.

[24] H. Hoppe. Efficient implementation of progressive meshes. *Computers and Graphics*, 22(1):27–36, 1998.

[25] M.-K. Hu. Visual pattern recognition by moment invariants. *IRE Transactions on Information Theory*, February:179–187, 1962.

[26] T. Huysmans, J. Sijbers, and B. Verdonk. Parameterization of tubular surfaces on the cylinder. In preparation.

[27] D. N. Kennedy, J. Sacks, P. A. Filipek, and V. S. Caviness. Three-dimensional Fourier shape analysis in magnetic resonance imaging. In *Annual International Conference of the IEEE Engineering in Medicine and Biology Society*, volume 12/1, pages 78–79, Philadelphia, USA, October 1990.

[28] V. Kindratenko and P. van Espen. Classification of irregularly shaped micro-objects using complex Fourier descriptors. In *ICPR96*, page B75.14, 1996.

[29] F. P. Kuhl and C. R. Giardina. Elliptic Fourier features of a closed contour. *Computer Graphics and Image Processing*, 18:236–258, 1982.

[30] S. Kuthirummal, C.V. Jawahar, and P.J. Narayanan. Fourier domain representation of planar curves for recognition in multiple views. *PR*, 37(4):739–754, April 2004.

[31] Pete E. Lestrel. *Fourier Descriptors and their Applications in Biology*. Cambridge University Press, 1997.

[32] S.X. Liao and M. Pawlak. On image analysis by moments. *IEEE Trans. Pattern Anal. Machine Intel.*, 18(3):254–266, 1996.

[33] S.X. Liao and M. Pawlak. On the accuracy of Zernike moments for image analysis. *IEEE Trans. Pattern Analysis and Machine Intell.*, 20(12):1358–1364, 1998.

[34] C. C. Lin and R. Chellappa. Classification of partial 2-D shapes using Fourier descriptors. *IEEE Transactions on Pattern Analysis and Machine Intelligence*, 9(5):686–690, September 1987.

[35] P. Milanfar, W.C. Karl, and A.S. Willsky. A moment-based variational approach to tomographic reconstruction. *IEEE Trans. Image Proc.*, 5:459–470, 1996.

[36] P. Milanfar, G.C. Verghese, W. Karl, and A.S. Willsky. Reconstructing polygons from moments with connections to Array processing. *IEEE Trans. Signal Proc.*, 43:432–443, 1995.

[37] R. Mukundan. A numerical approximation of two dimensional image moments. *Indian J. Pure Appl. Math.*, 22(10):879–886, 1991.

[38] E. Persoon and King-Sun Fu. Shape discrimination using Fourier descriptors. *IEEE Transactions on Systems, Man, and Cybernetics*, 7(3):629–639, 1977.

[39] Emil Praun and Hugues Hoppe. Spherical parametrization and remeshing. *ACM Transactions on Graphics*, 22(3):340–349, July 2003.

[40] R.J. Prokop and A.P. Reeves. A survey of moment-based techniques for unoccluded object representation and recognition. *CVGIP: Gaph. Models and Im. Proces.*, 54(5):438–460, 1992.

[41] C. W. Richard and H. Hemami. Identification of three-dimensional objects using Fourier descriptors of the boundary curve. *IEEE Transactions on Systems, Man, and Cybernetics*, 4(4):371–378, 1974.

[42] Y. Sato and I. Honda. Pseudodistance measures for recognition of curved objects. *IEEE Transactions on Pattern Analysis and Machine Intelligence*, 5(4):362–373, July 1983.

[43] M.I. Sezan and H. Stark. Incorporation of a priori moment information into signal recovery and synthesis problems. *J. Math. Anal. Appl.*, 122:172–186, 1987.

[44] J. Sijbers and D. Van Dyck. Efficient algorithm for the computation of 3D Fourier descriptors. In *Proceedings of the 3D Data Processing, Visualization and Transmission conference*, Padua, Italy, June 19-21 2002.

[45] V. Solachidis, N. Nikolaidis, and I.Pitas. Watermarking polygonal lines using Fourier descriptors. *IEEE Computer Graphics and Applications*, 24(3):44–51, 2004.

[46] L. H. Staib and J. S. Duncan. Deformable Fourier models for surface finding in 3D images. In *Proceedings of SPIE: Visualization in biomedical computing*, volume 1808, pages 90–104, 1992.

[47] V. Strakhov and M. Brodsky. On the uniqueness of the inverse logarithmic potential problem. *SIAM J. Appl. Math.*, 46:324–344, 1986.

[48] M.R. Teague. Image analysis via the general theory of moments. *J. Opt. Soc. Amer.*, 70(8):920–930, 1980.

[49] C.-H. Teh and R.T. Chin. On image analysis by the methods of moments. *IEEE Trans. Pattern Anal. Machine Intel.*, 10(4):496–512, 1988.

[50] T. P. Wallace and P. Wintz. An efficient, three-dimensional aircraft recognition algorithm using normalized Fourier descriptors. *Computer Graphics and Image Processing*, 3(1):99–126, 1980.

[51] J. Y. Wang and F. S. Cohen. Part II: 3D object recognition and shape estimation from image contours using B-splines shape invariant matching and neural network. *IEEE Transactions on Pattern Analysis and Machine Intelligence*, 16(1):1–12, 1994.

[52] Y. F. Wang, M. J. Magee, and J. K. Aggarwal. Matching three-dimensional objects using silhouettes. *IEEE Transactions on Pattern Analysis and Machine Intelligence*, 6(4):513–518, July 1984.

[53] M. F. Wu and H. T. Sheu. 3D invariant estimation of axisymmetric objects using Fourier descriptors. *Pattern recognition*, 29(2):267–280, 1996.

[54] M. F. Wu and H. T. Sheu. Computer vision and image analysis: Representation of 3D surfaces by two-variable Fourier descriptors. *IEEE Transactions on Pattern Analysis and Machine Intelligence*, 20(8):858–863, 1998.

[55] C. T. Zahn and R. Z. Roskies. Fourier descriptors for plane closed curves. *IEEE Transactions on Computers*, C-21:269–281, 1972.

[56] D. Zhang and G. Lu. A comparative study of three region shape descriptors. In D. Suter, R. Jarvis, and A. Bab-Hadiashar, editors, *DICTA2002: Digital Image Computing Techniques and Applications*, pages 1–6, 2002.